

## Small Molecule RPE65 Antagonists Limit the Visual Cycle and Prevent Lipofuscin Formation<sup>†</sup>

Pranab Maiti,<sup>‡</sup> Jian Kong,<sup>§</sup> So Ra Kim,<sup>§</sup> Janet R. Sparrow,<sup>§,||</sup> Rando Allikmets,<sup>§,||</sup> and Robert R. Rando<sup>\*,‡</sup>

Department of Biological Chemistry and Molecular Pharmacology, Harvard Medical School, Boston, Massachusetts 02115, and Departments of Ophthalmology and of Pathology and Cell Biology, Columbia University, New York, New York 10032

Received September 12, 2005; Revised Manuscript Received November 28, 2005

**ABSTRACT:** The accumulation of the lipofuscin fluorophores in retinal pigment epithelial (RPE) cells leads to the blinding degeneration characteristic of Stargardt disease and related forms of macular degeneration. RPE lipofuscin, including the fluorophore A2E, forms in large part as a byproduct of the visual cycle. Inhibiting visual cycle function with small molecules is required to prevent the formation of the retinotoxic lipofuscins. This in turn requires identification of rate-limiting steps in the operation of the visual cycle. Specific, non-retinoid isoprenoid compounds are described here, and shown through in both in vitro and in vivo experiments, to serve as antagonists of RPE65, a protein that is essential for the operation of the visual cycle. These RPE65 antagonists block regeneration of 11-*cis*-retinal, the chromophore of rhodopsin, thereby demonstrating that RPE65 is at least partly rate-limiting in the visual cycle. Furthermore, chronic treatment of a mouse model of Stargardt disease with the RPE65 antagonists abolishes the formation of A2E. Thus, RPE65 is also on the rate-limiting pathway to A2E formation. These nontoxic isoprenoid RPE65 antagonists are candidates for the treatment of forms of macular degeneration wherein lipofuscin accumulation is an important risk factor. These antagonists will also be used to probe the molecular function of RPE65 in vision.

The visual cycle is comprised of the biochemical reactions required for the regeneration of 11-*cis*-retinal, the chromophore of visual pigment in photoreceptor cells (1). In the sequence of events that initiates phototransduction, the 11-*cis*-retinal protonated Schiff base chromophore absorbs a photon of light and is isomerized to the all-*trans* configuration (2). The chemically reactive all-*trans*-retinal is subsequently cleared from the photoreceptor outer segment by retinol dehydrogenase-mediated reduction to vitamin A (3). The latter is subsequently transported to the retinal pigment epithelium (RPE)<sup>1</sup> where it is further processed to form 11-*cis*-retinal (Scheme 1) (1). Not all of the highly reactive all-*trans*-retinal generated in the photoreceptors is enzymatically reduced before it can chemically react with endogenous amines, including phosphatidylethanolamine (PE), to form the retinoid-derived fluorophores that constitute the lipofuscin of RPE (Scheme 1) (4). Thus, there is a bifurcation in the

pathway. Most of the all-*trans*-retinal generated is reduced by the RDH mentioned above. However, some of the chemically reactive all-*trans*-retinal partitions into a chemically mediated pathway that generates a set of photoreactive fluorogenic molecules. These fluorophores, which include A2E, photoisomers of A2E, and an all-*trans*-retinal dimer conjugate, are highly toxic to cells (5–7). Accordingly, the excessive accumulation of these compounds is considered the primary cause of RPE atrophy in recessive Stargardt disease (STGD), a juvenile form of macular degeneration (8, 9). STGD and other diseases, such as cone–rod dystrophy (CRD) and atypical retinitis pigmentosa (RP19), are caused by mutations in *ABCR*, the gene encoding the photoreceptor-specific ATP-binding cassette (ABC) transporter (10).

It is thought that *ABCR* transports all-*trans*-retinal–PE conjugates to the cytosolic side of the disk membrane for reduction by RDH (11, 12). *Abcr*-mediated translocation is clearly important for the removal of all-*trans*-retinal, since in the *Abcr* knockout (*Abcr*<sup>−/−</sup>) mouse, a model of STGD, levels of RPE lipofuscin fluorophores, such as A2E, are profoundly increased (12).

The evidence gleaned from studies of both human patients and animal models indicates that the excessive accumulation of A2E and related fluorophores plays a direct and essential role in the causation of the *ABCR*-associated disease. It follows that inhibition of A2E formation in diseases caused by *ABCR* defects, by limiting the visual cycle and, therefore, the formation of all-*trans*-retinal, represents a therapeutic approach to the treatment of AMD. A specific antagonist directed against a rate-limiting element in the visual cycle could emerge as a preventative, lipitor-like drug for the treatment of retinal degenerative disorders.

<sup>†</sup> The studies were funded, in part, by NIH Grants EY-015425 (R.R.R.) and EY12951 (J.R.S.) and Research to Prevent Blindness (J.R.S. and R.A.).

\* To whom correspondence should be addressed. Phone: (617) 432-1794. Fax: (617) 432-0471. E-mail: robert\_rando@hms.harvard.edu.

<sup>‡</sup> Harvard Medical School.

<sup>§</sup> Department of Ophthalmology, Columbia University.

<sup>||</sup> Department of Pathology and Cell Biology, Columbia University.

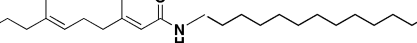
<sup>1</sup> Abbreviations: 13-RA, 13-*cis*-retinoic acid; AMD, age-related macular degeneration; CRD, cone–rod dystrophy; DMSO, dimethyl sulfoxide salt; DTT, dithiothreitol; EDTA, ethylenediaminetetraacetic acid; ERG, electroretinogram; IMH, isomerohydrolase; LRAT, lecithin retinol acyl transferase; mRPE65, membrane-bound RPE65; PBS, phosphate-buffered saline; PE, phosphatidylethanolamine; RDH, retinol dehydrogenase; RP19, atypical retinitis pigmentosa; RPE, retinal pigment epithelium; STGD, Stargardt disease; sRPE65, soluble RPE65; TDH, 3,7,11-trimethyldodeca-2,6,10-trienoic acid hexadecylamide; TDT, 13,17,21-trimethyldocosa-12,16,20-trien-11-one; tRP, all-*trans*-retinyl palmitate.

[illegible]

Our approach to both studying the temporal role of RPE65 in the operation of the visual cycle and exploring its role in the accumulation of lipofuscins in the A2E series was to

**t-Ret**
**Linker**
**Hydrophobe**

**K<sub>D</sub>=47 nM (tRP)**



Scheme 2 shows the three elements of an all-*trans*-retinyl ester, illustrated here by tRP, that are likely to be important for binding to mRPE65 (29). The retinoid moiety can be substituted with various isoprenoids, such as (*E,E*)-farnesyl palmitate, which binds with approximately the same affinity as does tRP itself (29). In addition, both ketones and amides can replace the ester moiety as a linker (29). Consequently, we designed and synthesized the two (*E,E*)-farnesyl-containing analogues (TDH and TDT) shown in Scheme 3 as antagonists of mRPE65. Molecules of this type should allow us to avoid the pleiotropic effects of retinoids and be more selective in their actions. It is shown here that the two mRPE65 antagonists powerfully inhibit visual cycle function *in vivo* and profoundly reduce the level of lipofuscin accumulation in the mouse model of STGD. These studies provide strong evidence that mRPE65 is rate-limiting in visual cycle function and in A2E formation and that mRPE65 is a valid target for therapies designed to prevent the accumulation of lipofuscin and possibly the onset and progression of macular degeneration.

Frozen bovine eye cups devoid of retinas were purchased from W. L. Lawson Co. (Lincoln, NE). Ethylenediamine-

tetraacetic acid (EDTA), phenyl-Sepharose CL-4B, Trizma base, *trans,trans*-farnesol, pyridinium chlorochromate, Dess–Martin reagent, decylmagnesium bromide, hexadecylamine, and dimethyl sulfoxide were from Sigma-Aldrich. Dithiothreitol (DTT) was from ICN Biomedicals Inc. Anagrade CHAPS was from Anatrace. HPLC grade solvents were from Sigma-Aldrich Chemicals. Anti-RPE65 (NFITKVNPELTETIK) antibody was obtained from Genmed Inc. Broad-spectrum EDTA-free protease inhibitor cocktail was obtained from Roche Biosciences. The precast gels (4–20%) for SDS–PAGE with BenchMark prestained molecular weight markers were from Invitrogen. DEAE-Sepharose was from Amersham Biosciences. All reagents were analytical grade unless specified otherwise.

## Methods

**Animal Studies.** Protocols were approved by the Standing Committee on Animal Care of Harvard Medical School and the Institutional Animal Care and Use Committee of Columbia University and complied with guidelines set forth by The Association for Research in Vision and Ophthalmology. Seven-week-old male Balb/c albino mice and 7-week-old male Sprague-Dawley rats were from Charles River Breeding Laboratories and were housed in a 12 h–12 h light–dark cycle. Eight- to ten-week-old *Abcr* null mutant mice (129/SV  $\times$  C57BL/6J) were bred as formerly described (12, 22), and *Abcr*<sup>−/−</sup> (knockout) and *Abcr*<sup>+/+</sup> (wild-type) mice were raised under 12 h on–off cyclic lighting with an in-cage illuminance of 30–50 lux. In *Abcr*<sup>−/−</sup> and *Abcr*<sup>+/+</sup> mice, *Rpe65* was sequenced as reported previously (22).

**Purification of mRPE65.** mRPE65 was extracted and purified from the bovine eye cups using a procedure described previously (32). Protein purity was established by silver staining and Western blotting (1:4000 primary antibody for 1 h at room temperature and 1:4000 secondary antibody for 0.5 h at room temperature). RPE65 solutions were concentrated with an Amicon Ultra centrifugal filtration device (30 kDa cutoff) from Millipore Corp. The final protein solution contained 100 mM phosphate-buffered saline (150 mM NaCl) (pH 7.4) and 1% CHAPSO. The protein concentration was measured by a modified Lowry method (33) using the Bio-Rad DC protein assay protocol.

**Syntheses.** (1) *13,17,21-Trimethyldocosa-12,16,20-trien-11-one (TDT)*. A solution of *trans,trans*-farnesol (200 mg, 0.9 mmol) in ether (2 mL) was added to a solution of decylmagnesium bromide (1 M solution in ether, 1.5 mL) at 0 °C and the mixture stirred for 15 min. The reaction mixture was then warmed to room temperature and the reaction quenched with aqueous saturated NH<sub>4</sub>Cl (1 mL). H<sub>2</sub>O (2 mL) was added, and the reaction mixture was extracted with hexane (3  $\times$  5 mL). The combined extracts were collected, washed with brine, dried with magnesium sulfate, and evaporated under reduced pressure. The residue was chromatographed (SiO<sub>2</sub>, EtOAc/light petroleum, 10:90) to give the alcohol (319 mg, 92%): *R*<sub>f</sub> (EtOAc/light petroleum, 2:8) = 0.56. Dess–Martin periodinate (419 mg, 0.99 mmol) was added to a solution of the above alcohol (319 mg, 0.83 mmol) in CH<sub>2</sub>Cl<sub>2</sub> (1.5 mL) at room temperature and the mixture stirred for 10 min. The reaction mixture was then treated with a sodium thiosulfate/sodium bicarbonate solution [1:1 (v/v) mixture of 10% sodium thiosulfate

and aqueous saturated NaHCO<sub>3</sub>, 3 mL], and stirring was continued for an additional 10 min. H<sub>2</sub>O (2 mL) was added; the reaction mixture was extracted with hexane (3  $\times$  5 mL), washed with brine, and dried with Mg<sub>2</sub>SO<sub>4</sub>, and the combined extracts were evaporated under reduced pressure. The residue was chromatographed (SiO<sub>2</sub>, EtOAc/light petroleum, 1:99) to give the ketone (TDT) (283 mg, 89%): *R*<sub>f</sub> (EtOAc/light petroleum, 2:8) = 0.8; <sup>1</sup>H NMR (200 MHz, CDCl<sub>3</sub>)  $\delta$  6.04 (s, 1H), 5.19–5.01 (m, 2H), 2.44–2.30 (m, 2H), 2.20–1.85 (m, 8H), 1.71 (s, 3H), 1.59 (s, 6H), 1.55 (s, 3H), 1.38–1.17 (m, 21H); ESI found *m/z* 383.3277 (M + Na), C<sub>25</sub>H<sub>44</sub>O requires *m/z* 383.3284 (M + Na).

(2) *3,7,11-Trimethyldodeca-2,6,10-trienoic Acid Hexadecylamide (TDH)*. NaCN (31 mg) and MnO<sub>2</sub> (590 mg) were added to a stirring solution of *trans,trans*-farnesol (100 mg, 0.45 mmol) in hexane (3 mL) at room temperature, followed by hexadecylamine (545 mg, 2.2 mmol), and stirring was continued for 1 h. An additional portion of MnO<sub>2</sub> (590 mg) was added and the mixture left overnight at room temperature with stirring. The mixture was then filtered through a pad of silica and Celite and washed with hexane several times. The combined extracts were evaporated, and the residue was chromatographed (SiO<sub>2</sub>, EtOAc/light petroleum, 3:97) to give 3,7,11-trimethyldodeca-2,6,10-trienoic acid hexadecylamide (145 mg, 70%): *R*<sub>f</sub> (EtOAc/light petroleum, 2:8) = 0.52; <sup>1</sup>H NMR (200 MHz, CDCl<sub>3</sub>)  $\delta$  8.18 (d, *J* = 9 Hz, 1H), 6.0 (d, *J* = 9.6 Hz, 1H), 5.2–5.0 (m, 2H), 3.42 (t, *J* = 6.8 Hz, 2H), 2.23–1.91 (m, 8H), 1.67 (s, 3H), 1.59 (s, 9H), 1.39–1.20 (m, 31H); ESI found *m/z* 482.4334 (M + Na), C<sub>31</sub>H<sub>57</sub>ON requires *m/z* 482.2332 (M + Na).

**Fluorescence Binding Assays.** RPE65 in PBS, with 1% CHAPS (pH 7.4), was used in the fluorometric titration studies. All titrations were performed at 25 °C. The samples in PBS buffer were excited at 280 nm, and the fluorescence was scanned from 300 to 500 nm. Fluorescence measurements, using 450  $\mu$ L quartz cuvettes with a path length of 0.5 cm, were taken at 25 °C on a Jobin Yvon Instruments Fluoromax 2 instrument employing the right-angle detection method.

The fluorescence of the protein solution was measured after equilibrating it at 25 °C for 10 min. The sample was then titrated with a solution of retinoid dissolved in DMSO in the absence of any overhead light, and the solution was mixed thoroughly before fluorescence measurements were taken. In each titration, to a 350  $\mu$ L solution of the protein was added an equivalent amount of ligand, typically 0.3  $\mu$ L, and the solution was thoroughly mixed before being allowed to equilibrate for 10 min prior to the recording of the fluorescence intensity. The addition of DMSO (0.1% per addition) did not have any effect on the fluorescence intensity. The binding constant (*K*<sub>D</sub>) was calculated from the fluorescence intensity as described before (17, 19).

**Electroretinogram (ERG) Determinations.** Mice were dark-adapted overnight before all ERG experiments. To determine the acute effect of compounds under study, mice were given a single intraperitoneal injection of a compound at 50 mg/kg in 25  $\mu$ L of DMSO under dim red light and kept in darkness for an additional 1 h before being exposed to the bleaching light prior to ERG recordings. Control (“untreated”) animals were injected with 25  $\mu$ L of vehicle (DMSO). Mice were anesthetized with ketamine (80 mg/kg) and xylazine (5–10 mg/kg), and pupils were dilated with



1% phenylephrine and 1% cyclopentolate, followed by an exposure to 5000 lux of bleaching light for 2 min. Under these conditions, >90% of the rhodopsin is bleached.

The ERG was recorded from the cornea with cotton wick saline electrodes for ~50 min immediately after bleaching. Subcutaneous 30 gauge needles on the forehead and trunk were used as reference and ground electrodes, respectively. The animals rested on a heater which kept their body temperature at 37 °C. The light stimulus was obtained from a Ganzfeld stimulator having a stroboscope (PS33 Grass Instruments Inc., West Warwick, RI) removed from its housing and recessed above and behind the head of the mouse. The flash was diffused to cover the Ganzfeld homogeneously. Maximum flash intensity was measured with a calibrated light meter (J16 Tektronics Instruments, Beaverton, OR). Responses were averaged by a Macintosh computer-controlled data acquisition system (PowerLab, AD Instruments, Mountain View, CA) at a frequency of 0.1 Hz.

The same animals were subjected to ERG experiments according to exactly the same protocol 3 days later, except no (repeated) injection of compounds was performed.

**Drug Treatment and Retinoid Extraction.** The drugs were injected intraperitoneally in DMSO as the carrier. Controls received DMSO alone. The volume of the solution was 50  $\mu$ L for mice and 180  $\mu$ L for rats. After the injections were given, the animals were housed in the dark for 2 h and then bleached for 2 h. Under these conditions, >90% of the rhodopsin is bleached.

Then the animals were dark-adapted (5 min for mice and 30 min for rats) before being sacrificed, and eyes were enucleated. In the experiments, male Balb/c mice and male Sprague-Dawley rats were used.

Eyes were placed in glass–glass homogenizer in 0.8 mL of 1 M hydroxylamine, 0.1 M MOPS [3-(*N*-morpholino)-propanesulfonic acid] (pH 6.5), and 0.2% SDS and homogenized (34). Ethanol (0.6 mL) was added, and the homogenates were incubated for 30 min at room temperature to allow formation of the 11-*cis*-retinal oximes (34). The retinoids were extracted with dichloromethane (3  $\times$  0.4 mL). The combined extracts were dried with magnesium sulfate, evaporated under the flow of argon, and subjected to HPLC analysis. The normal phase HPLC column was a YMC-PVA SIL NP, 250 mm  $\times$  4.6 mm column, and the mobile phase was a hexane/dioxane mixture (93:7, v/v) with a flow rate of 1.5 mL/min. Absorbance was monitored at 325 nm, and peaks were identified by comparison with standards. In the HPLC profiles that are shown, retinyl esters and 11-*cis*-retinal *syn*-oxime were measured. The regeneration time was 5 min with mice and 30 min with rats. The rates of regeneration and the effects of the drugs appeared indistinguishable between the Balb/c mice and the pigmented wild-type (129/SV  $\times$  C57BL/6J) mice (on the same genetic background as the Abcr knockout mice).

**Tissue Extraction and HPLC Analysis.** Posterior eye cups were pooled and homogenized in PBS using a tissue grinder. An equal volume of a mixture of chloroform and methanol (2:1) was added, and the sample was extracted three times. To remove insoluble material, extracts were filtered through cotton and passed through a reverse phase (C18 Sep-Pak, Millipore) cartridge with 0.1% TFA in methanol. After the solvent had been removed by evaporation under argon gas, the extract was dissolved in methanol containing 0.1% TFA,

for HPLC analysis. For quantification of A2E, a Waters Alliance 2695 HPLC system was employed with an Atlantis dC18 column (Waters, 4.6 mm  $\times$  150 mm, 3  $\mu$ m) and the following gradient of acetonitrile in water (containing 0.1% trifluoroacetic acid): 90 to 100% from 0 to 10 min and 100% acetonitrile from 10 to 20 min, with a flow rate of 0.8 mL/min with monitoring at 430 nm. The injection volume was 10  $\mu$ L. Extraction and injection for HPLC were performed under dim red light. Levels of A2E and iso-A2E were determined by reference to an external standard of HPLC-purified A2E/iso-A2E. Since A2E and iso-A2E reach photoequilibrium *in vivo* (4), use of the term A2E will refer to both isomers, unless stated otherwise.

## RESULTS

### *In Vitro Binding Activities of Specific mRPE65 Antagonists*

In previous quantitative fluorescence studies, we showed that mRPE65 saturably binds all-*trans*-retinyl palmitate (tRP) with a  $K_D$  of 47 nM (17, 19). Further structure–activity studies on binding of ligand to mRPE65 reveal that amide and ketone equivalents of tRP bound approximately as well as tRP itself (29). Moreover, isoprenoids, such as C15 farnesyl, can substitute for the all-*trans*-retinyl moiety (29). On the basis of these observations, we prepared the *trans*-,*trans*-farnesylated ketone (TDT) and amide (TDH), both shown in Scheme 3. The binding of the two analogues to mRPE65 was assessed using standard fluorescence methods (29). TDT and TDH were found to specifically bind to purified bovine mRPE65 as shown in Figure 1A,B. TDT is the more potent ligand and binds with a  $K_D$  of  $58 \pm 5$  nM, while TDH binds with a  $K_D$  of  $96 \pm 14$  nM. In these experiments, we made use of the fact that the specific binding of these analogues to mRPE65 quenches protein fluorescence. The potency of binding of these analogues is in the range expected from our previous binding studies (29).

### *In Vivo Studies with Analogues TDT and TDH*

**Acute Effects.** To determine whether TDT and TDH have an effect on the visual cycle *in vivo*, the overnight dark-adapted *Abcr*<sup>+/+</sup> (Rpe65 450Leu, pigmented, 129/SV  $\times$  C57BL/6J) mice received single (intraperitoneal) injections of the two compounds in separate experiments at 50 mg/kg. For comparison, mice were also injected with 13-*cis*-retinoic acid (13-RA; Accutane) at the same concentration. One hour after the treatment, the mice were subjected to photobleaching (5000 lux for 2 min to bleach ~90% of rhodopsin) and ERGs were recorded.

Figure 2A shows the effects of TDT and TDH on the ERG b-wave amplitudes in animals 1 h after treatment. Both isoprenoids delayed the recovery of dark-adapted visual responses to an extent similar to that of 13-RA as judged from dark-adapted ERG b-wave amplitudes recorded using dim light flashes delivered immediately before and at regular intervals after photobleaching. A substantial effect on rod b-wave recovery induced by TDT and TDH was still present 3 days after treatment, while no sustained effect of 13-RA was detected (Figure 2B).

To establish whether recovery of the dark-adapted rod b-wave was retarded because of an effect on 11-*cis*-retinal synthesis, we studied the effects of TDT on 11-*cis*-retinal

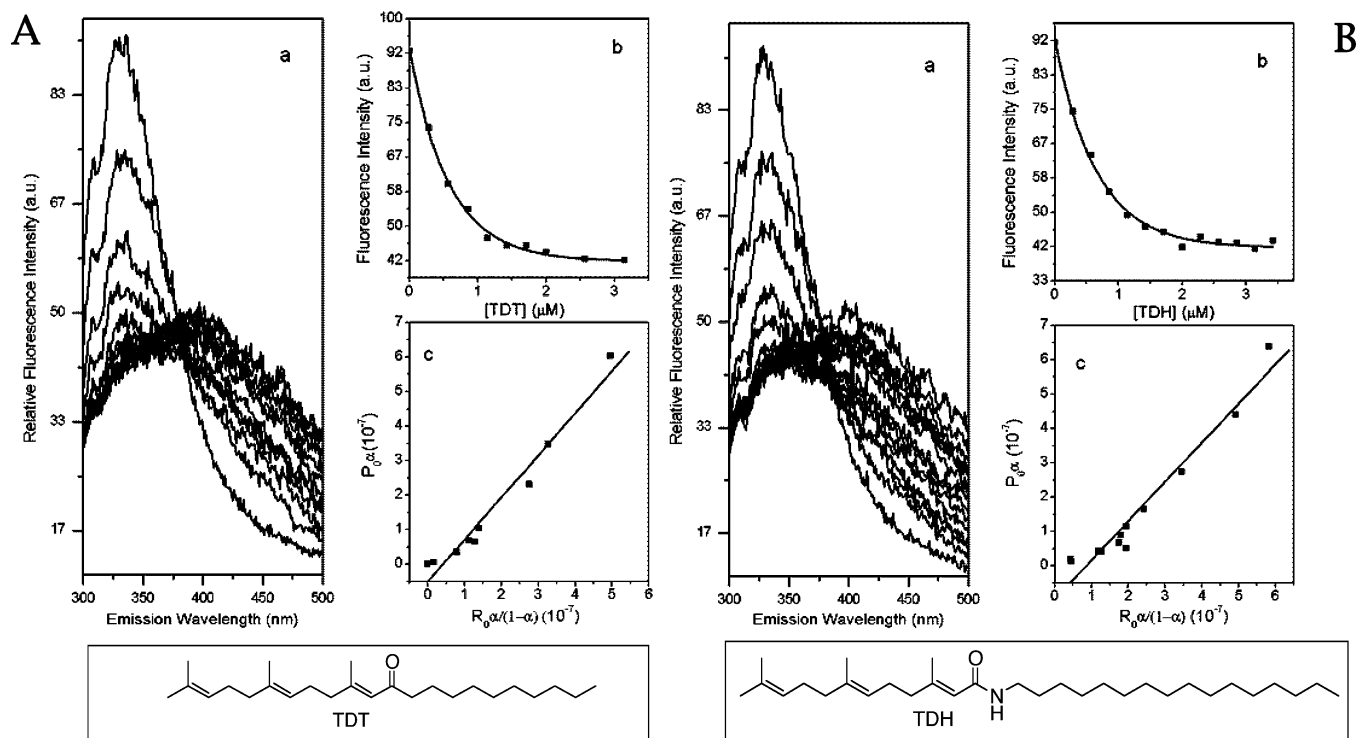


FIGURE 1: Fluorescence titration of mRPE65 with TDT and TDH. The excitation wavelength was at 280 nm, and the emission was observed through a 0.5 cm layer of solution. The titration solution consisted of 0.952  $\mu\text{M}$  mRPE65 in 100 mM phosphate-buffered saline (150 mM NaCl) (pH 7.4) and 1% CHAPS. For each compound, panel a shows the emission spectra of mRPE65 when binding to TDT or TDH. Panel b shows the change in the fluorescence intensity at 338 nm with increasing concentrations of TDT or TDH. Panel c shows the linear square fit plots of  $P_0\alpha$  vs  $R_0\alpha/(1-\alpha)$ , for the titration of mRPE65 vs TDT or TDH (17, 19).

regeneration in rats and mice. The 11-*cis*-retinal that is regenerated is essentially all bound to rhodopsin in rodents, so measuring its level is equivalent to measuring the rhodopsin content (30). Initial experiments were performed on Sprague-Dawley rats because similar experiments using 13-RA were previously carried out using these animals so that ready comparisons of potency and effectiveness can be made (26). In these experiments, 13-RA was shown to exhibit profound effects on visual cycle function by interfering with 11-*cis*-retinal regeneration after a bleaching (26). Accordingly, in the current experiments, the rats were given single injections (intraperitoneal) of TDT or TDH (50 mg/kg in DMSO), 13-RA (50 mg/kg in DMSO), and DMSO alone. After the analogues were injected, the rats were dark-adapted for 2 h and then exposed to light that led to <10% dark-adapted 11-*cis*-retinal in these animals, compared to dark-adapted controls (data not shown). The dark-adapted (2 h) animals in these experiments had approximately 85% 11-*cis*-retinal, as determined by these measurements. The remaining retinoids that were measured were in the retinyl ester pool (data not shown). After the bleached rats were allowed to dark-adapt again for 30 min, the animals were sacrificed, and the amount of regenerated 11-*cis*-retinal was determined as indicated in Methods. In these experiments, the amount of resynthesized 11-*cis*-retinal, the chromophore of rhodopsin, is measured by HPLC and compared to the amounts of all-*trans*-retinyl ester precursor. These one-point measurements provide a rough estimate of the relative abilities of the drug-treated animals to resynthesize 11-*cis*-retinal after bleaching (26). As shown in Figure 3A–C, both 13-RA and TDT achieved substantial (4–5-fold) inhibition of 11-*cis*-retinal regeneration. The inhibitory effect of TDH

is less pronounced than with TDT, as shown in Figure 3C. This is consistent with the observed lower potency of TDH as an mRPE65 antagonist compared to TDT. Upon repetition of the experiments two further times, the average inhibition values are as follows:  $78 \pm 2\%$  for 13-RA,  $79 \pm 4\%$  for TDT, and  $55 \pm 2\%$  for TDH. These percent inhibition values are generated by comparing the integrated areas under the retinyl ester and 11-*cis*-retinal *syn*-oxime peaks (Experimental Procedures).

It is significant that the size of the all-*trans*-retinyl ester pool increases at the expense of the 11-*cis*-retinal pool in the presence of TDT and TDH (Figure 3). The concomitant increase in the size of the all-*trans*-retinyl ester pool is expected of an antagonist of mRPE65. The magnitude of inhibition by 13-RA is approximately the same as that reported previously (26). In the case of 13-RA inhibition, the ester pool is a mixture of the 11-*cis* and all-*trans* isomers because of the inhibition of 11-*cis*-retinol dehydrogenase (25, 26). In the experiments described here with the isoprenoid antagonists, only all-*trans*-retinyl esters are detectable (data not shown).

Similar experiments with inhibitors were also performed in Balb/c mice. Here again inhibition is observed, but the effects are less pronounced than in rats, with both 13-RA and the isoprenoid antagonists. The inhibition values are as follows:  $33 \pm 4\%$  for 13-RA,  $35 \pm 2\%$  for TDT, and  $24 \pm 6\%$  for TDH. It is noteworthy that in rats the 11-*cis* chromophore is regenerated considerably more slowly than in mice (30). In mice, as in rats, the isoprenoid mRPE65 antagonists and 13-RA proved to be approximately equipotent with respect to the inhibition of 11-*cis*-retinal regeneration.

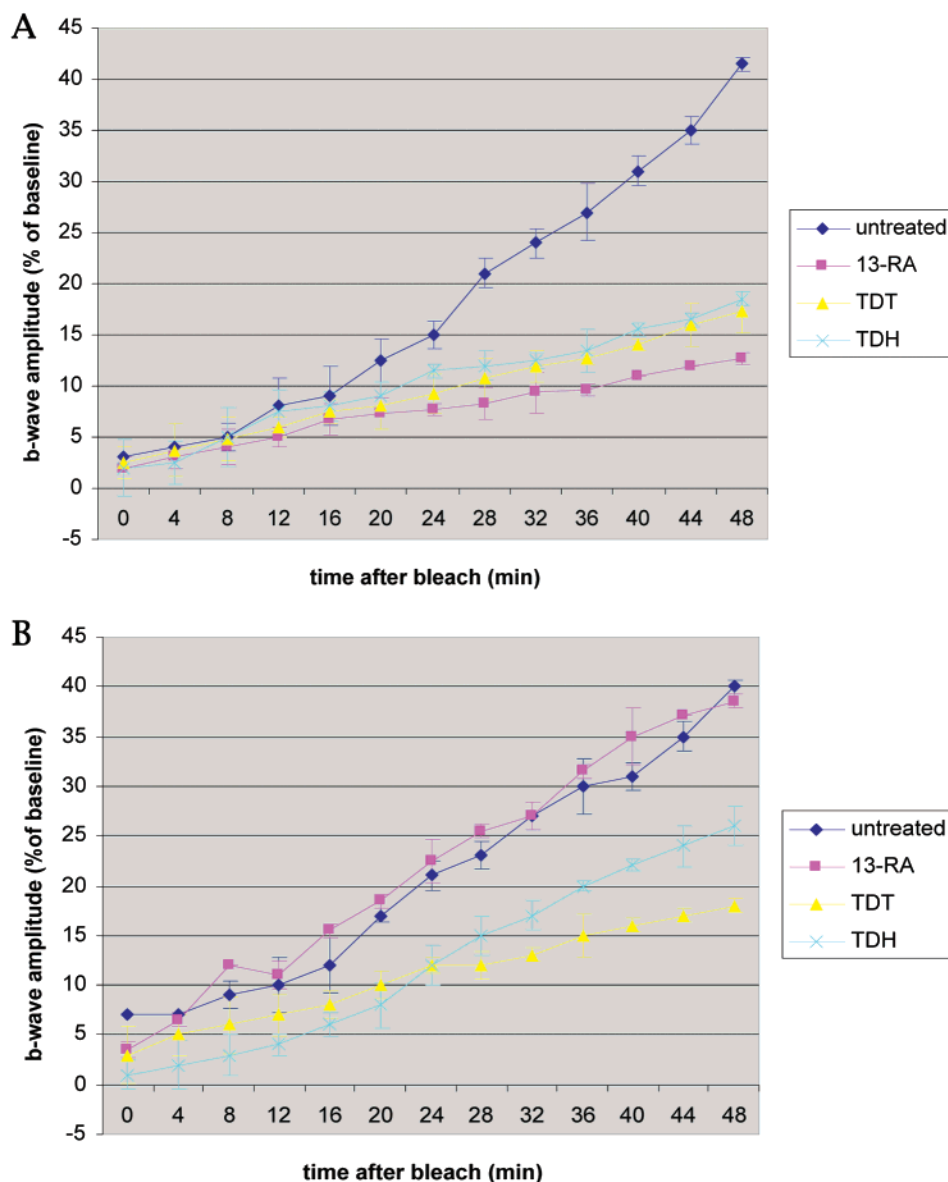


FIGURE 2: (A) Acute effect (1 h after treatment with a 50 mg/kg dose) of three compounds (13-RA, TDT, and TDH) on rod b-wave amplitude recovery after photobleaching. Experiments were performed as described in Results and Experimental Procedures. Results are averaged from three mice in each group with standard deviation bars shown. (B) Effect of the three compounds (13-RA, TDT, and TDH) on rod b-wave amplitude recovery after photobleaching 3 days after treatment with a one-time dose of 50 mg/kg of each compound. Experiments were performed as described in Results and Experimental Procedures. Results are averaged from three mice in each group with standard deviation bars shown.

*Effect of the Long-Term (Chronic) Treatment of  $Abcr^{-/-}$  Mice with TDT and TDH on A2E Accumulation.* The RPE65 antagonists TDT and TDH were further tested for their abilities to reduce the accumulation of the RPE lipofuscin fluorophores A2E and iso-A2E. Beginning at 2 months of age,  $Abcr^{-/-}$  mice (on the same genetic background as the  $Abcr^{+/+}$  animals) were given intraperitoneal injections of the two compounds at 50 mg/kg twice a week, and A2E and iso-A2E levels were determined by quantitative HPLC after an additional 2 months. As shown in Figure 4, both compounds, but especially TDT, were highly efficient in lowering the level of A2E accumulation. Specifically, the levels of A2E in eye cups of mice treated with TDT were 85% lower than in vehicle-treated (DMSO)  $Abcr^{-/-}$  animals (Figure 4D). These results demonstrate that the mRPE65 antagonists TDT and TDH are effective in vivo and slow the rate of A2E accumulation by limiting visual cycle function.

To investigate TDT further, we treated  $Abcr^{-/-}$  mice for 1 month beginning at 10 weeks of age and compared A2E and iso-A2E accumulation in TDT-treated mice with the amounts of these pigments in untreated mice at 10 weeks of age and untreated mice at 14 weeks of age (Figure 4E). In the 14-week-old TDT-treated mice, the quantity of A2E was maintained at levels present at the start of treatment (10 weeks of age) and was 30% lower than in the untreated 14-week-old mice. Therefore, TDT treatment abolished the accumulation of the lipofuscins. Comparable results were obtained with TDT treatment for 2 months beginning at 10 weeks of age (Figure 4F). Specifically, A2E levels were reduced by 45% as compared to those in untreated mice.

## DISCUSSION

RPE65 is of central importance in the operation of the visual cycle and has been shown to be necessary for

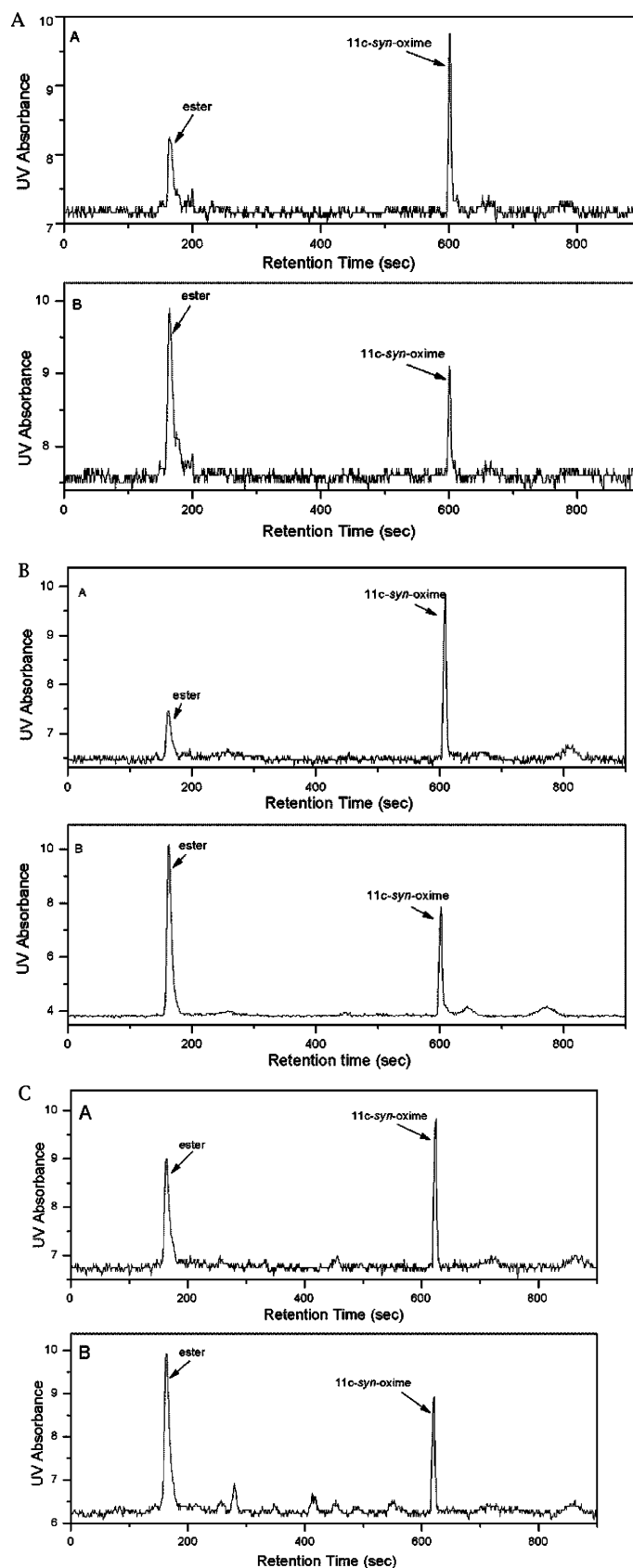


FIGURE 3: HPLC analysis of extracted retinoids from drug-treated rats. Experiments were carried out as described in Experimental Procedures. After the analogues were injected, the rats were dark-adapted for 2 h and then exposed to light that led to <10% of the dark-adapted 11-*cis*-retinal in these animals, compared to dark-adapted controls. Panel A shows HPLC data from 13-RA-treated Sprague-Dawley rats. In panel A, the relative amounts of 11-*cis*-retinal *syn*-oxime and all-*trans*-(*cis*)-retinyl esters are shown for the control (-13-RA) (top) and drug-treated animals (bottom). In panel B, the corresponding data are shown for the TDT-treated rats (top, control; bottom, TDT-treated). In this case, the ester pool in the drug-treated rat is largely, if not exclusively, all-*trans*. In panel C, the corresponding data are shown for the TDH-treated rats (top, control; bottom, TDH-treated). In this case, the ester pool in the drug treated rat is largely, if not exclusively, all-*trans*.



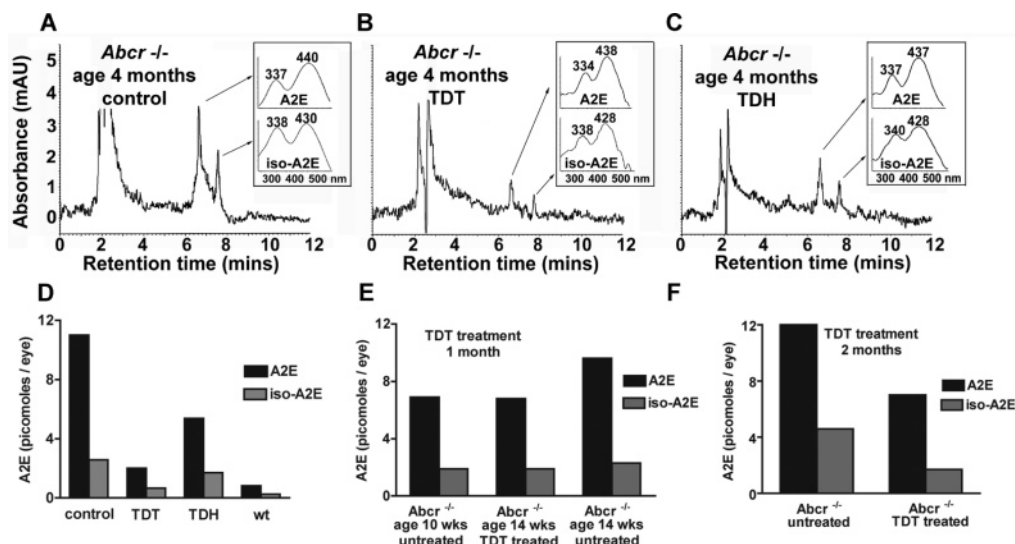


FIGURE 4: Quantitation of A2E and iso-A2E in eye cups of *Abcr*<sup>-/-</sup> mice. (A–C) Typical chromatograms obtained by reverse phase HPLC with monitoring at 430 nm illustrate the detection of A2E and iso-A2E and a reduction in peak intensity with TDT and TDH treatment relative to vehicle-treated controls. (D) A2E/iso-A2E quantitation following TDT and TDH treatment. *Abcr*<sup>-/-</sup> mice that were 2 months of age were treated with TDT or TDH (50 mg/kg twice weekly, intraperitoneally) for 2 months, and A2E and iso-A2E levels are compared to amounts in control (vehicle-only) eye cups and to amounts in wild-type mice. (E and F) *Abcr*<sup>-/-</sup> mice were treated with TDT (50 mg/kg twice weekly, intraperitoneally) for 1 (E) or 2 months (F) beginning at 10 weeks of age, and A2E and iso-A2E levels at the end of treatment (14 or 18 weeks of age) were compared to levels in 10-week-old vehicle-treated (control) mice and 14- or 18-week-old vehicle-treated (control) mice. A2E/iso-A2E levels were determined from HPLC chromatograms by integrating peak areas and normalizing to external standards. Values are expressed as picomoles per eye and are based on single samples obtained by pooling four eyes.

rhodopsin regeneration (15). The retinoic acids, which bind to mRPE65, block isomerization in RPE membranes (24). The fact that 13-RA also limits the visual cycle in rats *in vivo* (26) suggests the possibility that mRPE65 might be a viable target for interfering with visual cycle function. In rats, the effects of 13-RA on visual function are pronounced. There is an approximately 4-fold inhibition measured for 11-*cis*-retinal regeneration after bleaching (26). This inhibition is translated into a diminution in the accumulation of the lipofuscins in the A2E series in the *Abcr*<sup>-/-</sup> knockout mouse model (27). However, the retinoic acids exhibit pleiotropic effects and inhibit 11-*cis*-retinol dehydrogenase as well. We sought to prepare non-retinoid small molecule antagonists of mRPE65 to directly determine if inhibition of this target by itself could limit the visual cycle and establish that RPE65 function is part of the rate-limiting step in visual pigment regeneration. In addition, there was also the strong likelihood that inhibition of RPE65 might also interfere with the accumulation of the retinotoxic lipofuscins.

Two non-retinoid antagonists of mRPE65 were readily designed and shown to bind potently to mRPE65, a target unique to the visual cycle. Both TDT and TDH inhibited 11-*cis*-retinal regeneration after photobleaching to approximately the same extent as 13-RA. However unlike 13-RA, both TDT and TDH are directed solely at mRPE65, and *in vivo* inhibition results are consistent with this protein being the operant target. Rodents treated with TDT and TDH accumulate all-*trans*-retinyl esters behind the mRPE65 block. This result is expected, because the all-*trans*-retinyl esters are converted into 11-*cis*-retinol more slowly when mRPE65 is inhibited. By comparison, in the presence of 13-RA, the accumulation of both all-*trans*-retinyl and 11-*cis*-retinyl esters is noted (26). This occurs because 13-RA inhibits both mRPE65 and 11-*cis*-retinol dehydrogenase (25, 26). These results are entirely consistent with RPE65 being partly rate limiting in the operation of the visual cycle. The role of

RPE65 function in the accumulation of the lipofuscins in the A2E series was then explored.

Chronic treatment with TDT and TDH had profound effects on limiting A2E accumulation in the animal model of STGD, the *Abcr*<sup>-/-</sup> mouse. TDT, in particular, prevented A2E formation by approximately 85% compared to untreated *Abcr*<sup>-/-</sup> animals and brought A2E levels down to approximately those observed in wild-type animals of a similar age. In addition, and very importantly, TDT completely blocked the new accumulation of A2E in *Abcr*<sup>-/-</sup> mice. That is, the measured levels of A2E before and after TDT treatment were identical. This occurs even though visual cycle function was not even close to being completely inhibited. The relationship between the extent of inhibition of visual cycle turnover and A2E accumulation remains to be explored. It is likely to be nonlinear, at least in part due to the fact that A2E formation is second-order in all-*trans*-retinal. Other nonlinear effects may be operative as well.

With respect to the pharmacology of the isoprenoid mRPE65 antagonists, it should be noted that the effects of both TDT and TDH are substantially more persistent than with 13-RA, probably because they are more hydrophobic than the retinoic acids. An increase in hydrophobicity tends to slow rates of elimination of drugs. In addition, animals treated with TDT and TDH tolerated the compounds extremely well, showing no obvious signs of toxicity and/or distress, even when the compounds were administered every 48 h.

In conclusion, we have designed and studied specific, non-retinoid mRPE65 antagonists that inhibit 11-*cis*-retinal regeneration after bleaching, further supporting the hypothesis that mRPE65 is minimally part of the rate-limiting process in visual pigment regeneration. The analogues described here will be useful in a chemical genetic approach to the temporal function of mRPE65 in visual cycle function visual pigment regeneration. Similar analogues will be used



to probe the function of the congeneric sRPE65 as it relates to the regulation of the visual cycle (19). In addition to analyzing the function of RPE65 in vitro, we found the non-retinoid antagonists also profoundly inhibited lipofuscin A2E accumulation in the *Abcr*<sup>-/-</sup> mouse model of macular degeneration. Our studies suggest that these, or similar, molecules may be efficient and nontoxic candidates as drugs aimed at preventing the onset of lipofuscin-sensitive forms of macular degeneration, including STGD and a prevalent form of AMD (geographic atrophy) leading to visual loss (31).

## REFERENCES

- Lamb, T. D., and Pugh, E. N., Jr. (2004) Dark adaptation and the retinoid cycle of vision, *Prog. Retinal Eye Res.* 23, 307–380.
- Sakmar, T. P., Menon, S. T., Marin, E. P., and Awad, E. S. (2002) Rhodopsin: Insights from recent structural studies, *Annu. Rev. Biophys. Biomol. Struct.* 31, 443–484.
- Rattner, A., Smallwood, P. M., and Nathans, J. J. (2000) Identification and characterization of all-*trans*-retinol dehydrogenase from photoreceptor outer segments, the visual cycle enzyme that reduces all-*trans*-retinal to all-*trans*-retinol, *J. Biol. Chem.* 275, 11034–11043.
- Parish, C. A., Hashimoto, M., Nakanishi, K., Dillon, J., and Sparrow, J. (1998) Isolation and one-step preparation of A2E and iso-A2E, fluorophores from human retinal pigment epithelium, *Proc. Natl. Acad. Sci. U.S.A.* 95, 14609–14613.
- Sparrow, J. R., Nakanishi, K., and Parish, C. A. (2000) The lipofuscin fluorophore A2E mediates blue light-induced damage to retinal pigmented epithelial cells, *Invest. Ophthalmol. Visual Sci.* 41, 1981–1989.
- Mata, N. L., Weng, J., and Travis, G. H. (2000) Biosynthesis of a major lipofuscin fluorophore in mice and humans with ABCR-mediated retinal and macular degeneration, *Proc. Natl. Acad. Sci. U.S.A.* 97, 7154–7159.
- Fishkin, N. E., Sparrow, J. R., Allikmets, R., and Nakanishi, K. (2005) Isolation and characterization of a retinal pigment epithelial cell fluorophore: An all-*trans*-retinal dimer conjugate, *Proc. Natl. Acad. Sci. U.S.A.* 100, 7091–7096.
- Allikmets, R., Singh, N., Sun, H., Shroyer, N. F., Hutchinson, A., Chidambaram, A., Gerrard, B., Baird, L., Stauffer, D., Peiffer, A., Rattner, A., Smallwood, P., Li, Y., Anderson, K. L., Lewis, R. A., Nathans, J., Leppert, M., Dean, M., and Lupski, J. R. (1997) A photoreceptor cell-specific ATP-binding transporter gene (*ABCR*) is mutated in recessive Stargardt macular dystrophy, *Nat. Genet.* 15, 236–246.
- Allikmets, R., Shroyer, N. F., Singh, N., Seddon, J. M., Lewis, R. A., Bernstein, P. S., Peiffer, A., Zabriskie, N. A., Li, Y., Hutchinson, A., Dean, M., Lupski, J. R., and Leppert, M. (1997) Mutation of the Stargardt disease gene (*ABCR*) in age-related macular degeneration, *Science* 277, 1805–1807.
- Allikmets, R. (2000) Simple and complex ABCR: Genetic predisposition to retinal disease, *Am. J. Hum. Genet.* 67, 793–799.
- Beharry, S., Zhong, M., and Molday, R. S. (2004) N-Retinylidene-phosphatidylethanolamine is the preferred retinoid substrate for the photoreceptor-specific ABC transporter ABCA4 (*ABCR*), *J. Biol. Chem.* 279, 53972–53979.
- Weng, J., Mata, N. L., Azarian, S. M., Tzekov, R. T., Birch, D. G., and Travis, G. H. (1999) Insights into the function of Rim protein in photoreceptors and etiology of Stargardt's disease from the phenotype in *abcr* knockout mice, *Cell* 98, 13–23.
- Bavik, C. O., Eriksson, U., Allen, R. A., and Peterson, P. A. (1991) Identification and partial characterization of a retinal pigment epithelial membrane receptor for plasma retinol-binding protein, *J. Biol. Chem.* 266, 14978–14985.
- Hamel, C. P., Tsilou, E., Harris, E., Pfeffer, B. A., Hooks, J. J., Detrick, B., and Redmond, T. M. (1993) A developmentally regulated microsomal protein specific for the pigment epithelium of the vertebrate retina, *J. Neurosci. Res.* 34, 414–425.
- Redmond, T. M., Yu, S., Lee, E., Bok, D., Hamasaki, D., Chen, N., Goletz, P., Ma, J. X., Crouch, R. K., and Pfeiffer, K. (1998) RPE65 is necessary for production of 11-*cis*-vitamin A in the retinal visual cycle, *Nat. Genet.* 20, 344–351.
- Jahng, W. J., David, C., Nesnas, N., Nakanishi, K., and Rando, R. R. (2003) A cleavable affinity biotinylation agent reveals a retinoid binding role for RPE65, *Biochemistry* 42, 6159–6168.
- Gollapalli, D. R., Maiti, P., and Rando, R. R. (2003) RPE65 operates in the vertebrate visual cycle by stereospecifically binding all-*trans*-retinyl esters, *Biochemistry* 42, 11824–11830; (2004) *Biochemistry* 43, 7226 (erratum).
- Mata, N. L., Moghrabi, W. N., Lee, J. S., Bui, T. V., Radu, R. A., Horwitz, J., and Travis, G. H. (2004) RPE65 is a retinyl ester binding protein that presents insoluble substrate to the isomerase in retinal pigment epithelial cells, *J. Biol. Chem.* 279, 635–643.
- Xue, L., Gollapalli, D. R., Maiti, P., Jahng, W. J., and Rando, R. R. (2004) A palmitoylation switch mechanism in the regulation of the visual cycle, *Cell* 117, 761–771.
- Moiseyev, G., Chen, Y., Takahashi, Y., Wu, B. X., and Ma, J.-X. (2005) RPE65 is the isomerohydrolase in the retinoid visual cycle, *Proc. Natl. Acad. Sci. U.S.A.* 102, 12413–12418.
- Jin, M., Li, S., Moghrabi, W. N., Sun, H., and Travis, G. H. (2005) Rpe65 Is the Retinoid Isomerase in Bovine Retinal Pigment Epithelium, *Cell* 122, 449–459.
- Kim, S. R., Fishkin, N., Kong, J., Nakanishi, K., Allikmets, R., and Sparrow, J. R. (2004) RPE65 Leu450Met variant is associated with reduced levels of the retinal pigment epithelium lipofuscin fluorophores A2E and iso A2E, *Proc. Natl. Acad. Sci. U.S.A.* 101, 11668–11672.
- Lyubarsky, A. L., Savchenko, A. B., Morocco, S. B., Daniele, L. L., Redmond, T. M., and Pugh, E. N., Jr. (2005) Mole quantity of RPE65 and its productivity in the generation of 11-*cis*-retinal from retinal esters in the living mouse eye, *Biochemistry* 44, 9880–9888.
- Gollapalli, D. R., and Rando, R. R. (2004) The specific binding of retinoic acid to RPE65 and approaches to the treatment of macular degeneration, *Proc. Natl. Acad. Sci. U.S.A.* 101, 10030–10035.
- Law, W. C., and Rando, R. R. (1989) The molecular basis of retinoic acid induced night blindness, *Biochem. Biophys. Res. Commun.* 161, 825–829.
- Sieving, P. A., Chaudhry, P., Kondo, M., Provenzano, M., Wu, D., Carlson, T. J., Bush, R. A., and Thompson, D. A. (2001) Inhibition of the visual cycle in vivo by 13-*cis*-retinoic acid protects from light damage and provides a mechanism for night blindness in isotretinoin therapy, *Proc. Natl. Acad. Sci. U.S.A.* 98, 1835–1840.
- Radu, R. A., Mata, N. L., Nusinowitz, S., Liu, X., Sieving, P. A., and Travis, G. H. (2003) Treatment with isotretinoin inhibits lipofuscin accumulation in a mouse model of recessive Stargardt's macular degeneration, *Proc. Natl. Acad. Sci. U.S.A.* 100, 4742–4747.
- Guzzo, C. A., Lazarus, G. S., and Werth, V. P. (1996) in *Goodman and Gilman's: The Pharmacological Basis of Therapeutics*, 9th ed. (Hardman, J. G., and Limbird, L. E., Eds.) pp 1598–1602, McGraw-Hill, New York.
- Maiti, P., Gollapalli, D., and Rando, R. R. (2005) The specificity of all-*trans*-retinyl ester binding to RPE65, *Biochemistry* 44, 14463–14469.
- Van Hooser, J. P., Garwin, G. G., and Saari, J. C. (2000) Analysis of visual cycle in normal and transgenic mice, *Methods Enzymol.* 316, 565–575.
- Holz, F. G., Bellman, C., Staudt, S., Schmitt, F., and Volcker, H. E. (2001) Fundus autofluorescence and development of geographic atrophy in age-related macular degeneration, *Invest. Ophthalmol. Visual Sci.* 42, 1051–1056.
- Ma, J.-X., Zhang, J., Othersen, K. L., Moiseyev, G., Ablonczy, Z., Redmond, T. M., Chen, Y., and Crouch, R. K. (2001) Expression, purification, and MALDI analysis of RPE65, *Invest. Ophthalmol. Visual Sci.* 42, 1429–1435.
- Lowry, O. H., Rosebrough, N. J., Farr, A. L., and Randall, R. J. (1951) Protein measurement with the folin phenol reagent, *J. Biol. Chem.* 193, 265–275.
- Groenendijk, G. W. T., De Grip, W. J., and Daemen, F. J. M. (1980) Quantitative determination of retinals with complete retention of their geometric configuration, *Biochim. Biophys. Acta* 617, 430–438.

BI0518545